



Mabtech IRIS™
SPOT ANALYSIS REINVENTED

Read how >

MABTECH

Capture | Detect | Discover



The *Pseudomonas* Toxin Pyocyanin Inhibits the Dual Oxidase-Based Antimicrobial System as It Imposes Oxidative Stress on Airway Epithelial Cells

This information is current as of December 11, 2018.

Balázs Rada, Kristen Lekstrom, Sorin Damian, Corinne Dupuy and Thomas L. Leto

J Immunol 2008; 181:4883-4893; ;
doi: 10.4049/jimmunol.181.7.4883
<http://www.jimmunol.org/content/181/7/4883>

References This article **cites 41 articles**, 12 of which you can access for free at:
<http://www.jimmunol.org/content/181/7/4883.full#ref-list-1>

Why *The JI*? Submit online.

- **Rapid Reviews! 30 days*** from submission to initial decision
- **No Triage!** Every submission reviewed by practicing scientists
- **Fast Publication!** 4 weeks from acceptance to publication

**average*

Subscription Information about subscribing to *The Journal of Immunology* is online at:
<http://jimmunol.org/subscription>

Permissions Submit copyright permission requests at:
<http://www.aai.org/About/Publications/JI/copyright.html>

Email Alerts Receive free email-alerts when new articles cite this article. Sign up at:
<http://jimmunol.org/alerts>

The Journal of Immunology is published twice each month by
The American Association of Immunologists, Inc.,
1451 Rockville Pike, Suite 650, Rockville, MD 20852
Copyright © 2008 by The American Association of
Immunologists. All rights reserved.
Print ISSN: 0022-1767 Online ISSN: 1550-6606.



The *Pseudomonas* Toxin Pyocyanin Inhibits the Dual Oxidase-Based Antimicrobial System as It Imposes Oxidative Stress on Airway Epithelial Cells¹

Balázs Rada,* Kristen Lekstrom,* Sorin Damian,† Corinne Dupuy,‡ and Thomas L. Leto^{2*}

The dual oxidase-thiocyanate-lactoperoxidase (Duox/SCN⁻/LPO) system generates the microbicidal oxidant hypothiocyanite in the airway surface liquid by using LPO, thiocyanate, and Duox-derived hydrogen peroxide released from the apical surface of the airway epithelium. This system is effective against several microorganisms that infect airways of cystic fibrosis and other immunocompromised patients. We show herein that exposure of airway epithelial cells to *Pseudomonas aeruginosa* obtained from long-term cultures inhibits Duox1-dependent hydrogen peroxide release, suggesting that some microbial factor suppresses Duox activity. These inhibitory effects are not seen with the pyocyanin-deficient *P. aeruginosa* strain PA14 Phz1/2. We show that purified pyocyanin, a redox-active virulence factor produced by *P. aeruginosa*, inhibits human airway cell Duox activity by depleting intracellular stores of NADPH, as it generates intracellular superoxide. Long-term exposure of human airway (primary normal human bronchial and NCI-H292) cells to pyocyanin also blocks induction of Duox1 by Th2 cytokines (IL-4, IL-13), which was prevented by the antioxidants glutathione and *N*-acetylcysteine. Furthermore, we showed that low concentrations of pyocyanin blocked killing of wild-type *P. aeruginosa* by the Duox/SCN⁻/LPO system on primary normal human bronchial epithelial cells. Thus, pyocyanin can subvert *Pseudomonas* killing by the Duox-based system as it imposes oxidative stress on the host. We also show that lactoperoxidase can oxidize pyocyanin, thereby diminishing its cytotoxicity. These data establish a novel role for pyocyanin in the survival of *P. aeruginosa* in human airways through competitive redox-based reactions between the pathogen and host. *The Journal of Immunology*, 2008, 181: 4883–4893.

The respiratory system is a major exposure site for microbial entry into the body. As such, multiple mechanisms are responsible for preventing respiratory infections, including microbial detection systems, mucin and airway surface liquid (ASL)³ production, ciliary clearance, communication between epithelial cells and cells of innate and adaptive immunity, and production of antimicrobial compounds. One of the innate airway antimicrobial defense systems of renewed interest is the hydrogen peroxide-thiocyanate-lactoperoxidase (H₂O₂/SCN⁻/

LPO) system, in which LPO uses H₂O₂ to catalyze oxidation of the pseudohalide SCN⁻ into the microbicide hypothiocyanite (OSCN⁻): H₂O₂ + SCN⁻ → OSCN⁻ + H₂O. The toxicity of this system has long been appreciated in other exocrine secretions, such as milk (1) and saliva (2). Targets of the H₂O₂/SCN⁻/LPO system include *Streptococci*, *Staphylococci*, *Haemophilus influenzae* (3), *Pseudomonads*, *Escherichia coli* (4), and viral and fungal pathogens (5, 6). LPO is found in sheep airways at concentrations as high as 1% of total soluble protein and its inhibition results in reduced microbial clearance (7). Significant levels of LPO are also detected in human airway secretions (3). The primary substrate of LPO, SCN⁻, is present in human airway secretions at an average concentration of 0.46 mM (3), which exceeds amounts needed to support LPO activity (8). Thiocyanate is transported into the ASL by epithelial cells by at least three apical plasma membrane transporters: the cystic fibrosis transmembrane conductance regulator (CFTR) (9), Ca²⁺-activated chloride channels, and pendrin (SLC26A4) (10). Comparatively low levels of H₂O₂ are detected in human airways, in the 1–10 μM range (11), which may be due to antioxidant properties of abundant LPO.

Although the H₂O₂/SCN⁻/LPO system of exocrine secretions has been studied for years, the source of H₂O₂ remained unclear until we reported high expression of NADPH oxidases (Nox), dual oxidase (Duox) 1 and Duox2, in epithelial cells of exocrine glands and along mucosal surfaces (12). The dual oxidases were first detected in the thyroid gland and were proposed to serve as H₂O₂ sources needed to support thyroperoxidase activity during thyroid hormone biosynthesis (13, 14). Duox expression was also detected in other nonthyroid tissues, including salivary glands, bronchial and tracheal surfaces, and the gastrointestinal tract (12, 15). Based

*National Institutes of Health, National Institute of Allergy and Infectious Diseases, Laboratory of Host Defenses, Rockville, MD 20852; †Lonza Walkersville, Walkersville, MD 21793; and ‡Centre National de la Recherche Scientifique, FRE2939, Villejuif, France; Université Paris-Sud 11, Orsay, France; and Institut Gustave Roussy, Villejuif, France

Received for publication May 1, 2008. Accepted for publication July 21, 2008.

The costs of publication of this article were defrayed in part by the payment of page charges. This article must therefore be hereby marked *advertisement* in accordance with 18 U.S.C. Section 1734 solely to indicate this fact.

¹ This work was supported by funding through the Intramural Research Program of the National Institutes of Health, National Institute of Allergy and Infectious Diseases.

² Address correspondence and reprint requests to Dr. Thomas L. Leto, National Institutes of Health, National Institute of Allergy and Infectious Diseases, 12441 Parklawn Drive, Bethesda, MD, 20892. E-mail address: tlet@nih.gov

³ Abbreviations used in this paper: ASL, airway surface liquid; ALI, air-liquid interface; CF, cystic fibrosis; CFTR, cystic fibrosis transmembrane conductance regulator; DPI, diphenylene iodonium; Duox, dual oxidase; GSH, glutathione; int. RLU, integrated RLU; LB, Luria-Bertani; LPO, lactoperoxidase; MPO, myeloperoxidase; NAC, *N*-acetylcysteine; NHBE, normal human bronchial epithelial; Nox, NADPH oxidase; OSCN⁻, hypothiocyanite; PA14, *Pseudomonas aeruginosa* 14 strain; PAO1, *Pseudomonas aeruginosa* O1 strain; Pyo, pyocyanin; RLU, relative luminescence unit; ROS, reactive oxygen species; SCN⁻, thiocyanate; siRNA, small interfering RNA; WT, wild type.

on the parallel expression patterns of Duox and LPO in salivary glands, gastrointestinal tissues, and airways, we suggested a functional partnership of Duox in supporting antimicrobial activity of LPO in exocrine secretions (12). The Duox enzymes bind Ca^{2+} through their EF-hands and their activities are responsive to Ca^{2+} -mobilizing agonists. These oxidases require maturation factors (Duox activators, Duoxa1 and Duoxa2) to be transported to their final destination, the plasma membrane (16). In human major airways Duox is found in the surface epithelium (12), where it is concentrated along the apical aspect (Ref. 17 and T. Ueyama, K. Lekstrom and T. L. Leto, unpublished). LPO is produced in acinar pockets of submucosal glands of human airways, but it accumulates in the airway surface liquid layer (3, 12). Duox releases extracellular H_2O_2 from the apical surface of airway epithelial cells (17) where, together with SCN^- , it would effectively support LPO-mediated killing of airway pathogens. Recently, primary airway epithelial cells and tracheal explants of different mammalian origin were shown to kill *Pseudomonas aeruginosa* and *Staphylococcus aureus* in vitro in a Duox-, LPO- and SCN^- -dependent manner (18).

P. aeruginosa is an opportunistic pathogen of human airways that usually infects immunocompromised host (cystic fibrosis (CF), chronic obstructive pulmonary disease, pneumonia, burn, HIV, or cancer chemotherapy patients) (19). *P. aeruginosa* harbors a variety of cell-attached and extracellular virulence factors that are induced through quorum-sensing signals as a consequence of bacterial overgrowth and biofilm formation in chronically infected individuals. One of the secreted factors is pyocyanin (Pyo), a blue heterocyclic metabolite of phenazine compounds that is redox-active (reviewed in Ref. 20) and toxic against a range of host organisms. Many effects of Pyo on airway epithelial cells have been described; that is, it causes cellular senescence and ciliary dyskinesia, induces IL-8 secretion, decreases glutathione levels, and inhibits catalase activity (reviewed in Ref. 21). Despite this spectrum of effects, its redox activity is considered the primary basis for its action. Pyo is a zwitterion that easily crosses cell membranes; in the cytosol it reacts with reduced NADH or NADPH, becomes reduced, and donates an electron to molecular oxygen, thereby producing intracellular superoxide (O_2^-) anions (22).

Because Pyo and the dual oxidases share some of the same substrates (molecular oxygen and NADPH), we investigated possible competitive interactions of Pyo and Duox enzymes in human airway epithelial cells. We show herein that Duox1- and calcium-dependent H_2O_2 release by airway epithelial cells is abolished by prior exposure to *P. aeruginosa* obtained from long-term cultures. This was attributed to Pyo production by long-term cultures. Purified Pyo inhibits Duox activity and expression based on its ability to compete for intracellular NADPH and inflict oxidative stress on the host. Furthermore, we show that physiological levels of LPO can effectively detoxify Pyo. Thus, competitive redox reactions are involved in airway epithelial host defense against microbial infection, as well as in the microbe's counteroffensive adaptation to the host environment.

Materials and Methods

Primary human cells and cell lines

The human pulmonary carcinoma cell line, NCI-H292, was purchased from the American Type Culture Collection (ATCC; CRL-1848). Cells were grown in RPMI 1640 medium (Invitrogen) containing 10% FBS, 1% penicillin-streptomycin, 1% L-glutamine, 1% sodium-pyruvate, and 1% HEPES. The following cytokines were used: IL-4 (10 ng/ml), IL-13 (10 ng/ml), and IFN- γ (1 U/ml) (recombinant human, R&D Systems).

Primary normal human bronchial epithelial (NHBE) cells were isolated from normal tissue at Lonza, cultured for one passage in 75-cm² Falcon flasks in bronchial/tracheal epithelial cell basal medium con-

taining all SingleQuot bronchial epithelial cell growth medium supplements, with the following modifications based on observations reported by Gray et al. (23): human epidermal growth factor (25 ng/ml; Collaborative Research), all-*trans* retinoic acid (5×10^{-8} M; Sigma-Aldrich), BSA (1.5 $\mu\text{g}/\text{ml}$; Sigma-Aldrich), bovine pituitary extract (1% (v/v) SingleQuot from Lonza), and gentamicin and amphotericin B (50 $\mu\text{g}/\text{ml}$). Upon reaching 80% confluence the cells were trypsinized and seeded onto 6- or 24-well polyester (0.4- μm pore) membrane transwells (Transwell-COL or Transwell Clear (Costar), precoated with rat tail collagen I (Collaborative Research)) at a density of $20\text{--}50 \times 10^3$ cells/cm². When cells reached confluence, the upper chamber medium was removed and the lower medium was replaced with air-liquid interface (ALI) medium composed of: 50% bronchial epithelial cell growth medium/50% DMEM, supplemented as above (Lonza). Cells were maintained in the ALI format as long as 28 days by feeding daily with ALI medium. After 1 wk of culture on ALI, the cells formed a sealed monolayer that exhibited transepithelial resistances >1000 Ohm/cm². Antibiotics were omitted from the culture medium 2 days before microbial killing experiments, typically on days 19–24.

K-562 cells were purchased from ATCC (CCL-243), transduced retrovirally with NADPH oxidase components (p47^{phox}, p67^{phox}, and gp91^{phox}), and then clonally selected for high levels of the reconstituted Nox2-based NADPH oxidase (referred to as K562⁺⁺⁺ cells; Ref. 24).

Bacterial strains

The following bacterial strains were used: *P. aeruginosa* ATCC 10145 (PA 10145; ATCC); PAO1 wild type (WT) (*Pseudomonas* Mutant Library, University of Washington, Seattle), PA14 WT and Pyo-deficient mutant PA14 PhzM (gift from Frederick M. Ausubel, Harvard Medical School, Boston, MA) (25), and the PA14 phenazine-deficient mutant Phz1/2 (provided by You-Hee Cho, Sogang University, Seoul, South Korea) (26). *Burkholderia cepacia* was a gift from Dr. Steven Holland (National Institute of Allergy and Infectious Diseases, National Institutes of Health). Bacteria were grown in Luria-Bertani (LB) broth (KD Medical) and incubated for up to 3 days (shaking, 37°C). Where mentioned, densities of the cultures were determined from absorbance at 600 nm.

Western blotting

Airway cells were washed three times with cold calcium- and magnesium-free PBS and then lysed by Nonidet P-40 lysis buffer (Boston Bioproducts) containing 150 μM PMSF (Fluka Biochemika) and 1% protease inhibitor cocktail (dissolved in DMSO; Sigma-Aldrich). Lysates were centrifuged and protein concentrations in supernatants were determined using the bicinchoninic acid assay (Pierce). Equal amounts of protein were loaded and electrophoresed on SDS-polyacrylamide gels (8%; Tris-glycine gel, Invitrogen). Gels were blotted on nitrocellulose membrane (Invitrogen) using the TransBlot SD semidry blotting cell (Bio-Rad). Blots were blocked overnight in TTBS (TBS buffer containing 5% milk powder and 0.05% Tween 20). Blots were incubated with primary Abs (room temperature, 1 h, TTBS), washed three times with TTBS and then probed with secondary HRP-linked Abs (room temperature, 1 h, TTBS). After repeated washes, blots were developed by chemiluminescence using the Lumigen DS detection kit (GE Healthcare). The primary Abs used in this study were: anti-Duox (rabbit, polyclonal; 1/2000) (15), anti- β -actin (rabbit, polyclonal, Sigma-Aldrich; 1/2000), and anti- α -tubulin (mouse, monoclonal, Santa Cruz Biotechnology; 1/2000). Secondary Abs used in this study were: HRP-linked anti-rabbit IgG from donkey (GE Healthcare; 1/1000) and HRP-linked anti-mouse IgG from sheep (GE Healthcare; 1/1000).

RNA interference

To silence gene expression by RNA interference, 5×10^5 NCI-H292 cells per well were seeded onto 6-well plates (BD Biosciences) 1 day before transfection. Cells were transfected at 20–30% confluence with either 50 or 100 nM Duox1-specific small interfering RNAs (siRNAs; Applied Biosystems) for 4 h in Opti-MEM medium (Invitrogen) using Lipofectamine 2000 transfection agent (Invitrogen). Cytokine treatment by IL-4 and IL-13 (each 10 ng/ml) was started immediately after transfection. Gene silencing efficiency was validated by Western blot analysis 72 h post-transfection. The following siRNAs were used (sequence of the sense strand): Duox1 No. 1: 5'-GGACUUAUCCUGGCUAGAG-3' (siRNA No. 24969); Duox1 No. 2: 5'-GGUAUUGAUCUGUCCUCU-3' (siRNA 108942); Duox1 No. 3: 5'-CCAUGUGUUGGUUGAAGAU-3' (siRNA 117547); Duox1 No. 4: 5'-GCUAUGCAGAUCCGUGUA-3' (siRNA 117546); β -actin: 5'-GAUGAGAUUGGCAUGGCU-3'; negative control: 5'-CCGUAUCGUAAGCAGUACU-3'.

Purification of Pyo

Pyo was prepared from supernatants of WT PA10145 and PA14 *P. aeruginosa* strains cultured for 2.5 days in LB medium. The filtered, bacterium-free culture supernatants were subjected to repeated chloroform extraction cycles, as described previously (27). In the first step, Pyo was extracted by adding chloroform to the crude supernatant, whereas the second aqueous extraction of the chloroform phase used acidified distilled water (pH 1.0). Subsequent chloroform extractions (repeated five times) required neutralization of the aqueous extracts. Final Pyo extracts were concentrated to 1–3 mM in distilled water and stored at 4°C in the dark. Pyo concentrations were determined based on an absorption coefficient of 2460 mM⁻¹ cm⁻¹ at 520 nm (protonated form at pH 1.0). The identity and purity of Pyo preparations were confirmed by mass spectrometry, revealing one major protonated species with a molecular mass of 211.08 (Mass Spectrometry Unit, Research Technologies Branch, National Institute of Allergy and Infectious Diseases, National Institutes of Health).

Measurement of H₂O₂ release

Extracellular H₂O₂ release was measured by a luminol/HRP-based chemiluminescence assay. Trypsinized NCI-H292 cells (1.5 × 10⁶/ml, 50 μl) were preincubated with or without 10 μM diphenylene iodonium (DPI) (37°C, 10 min) and were stimulated by addition of an equal volume of HBSS containing 1 mM luminol, 20 U/ml HRP, and agonist. Luminescence was measured in luminescence 96-well plate reader (Luminoskan Ascent, Thermo Scientific). This assay reports real-time production of H₂O₂ as reflected in the decay of oxidized luminol. The results are shown either as kinetics of H₂O₂ production, expressed as relative luminescence units (RLU) vs time, or as integrated luminescence (int. RLU), in absolute numbers or normalized.

Extracellular H₂O₂ generation was quantified by the Amplex Red/HRP assay (Molecular Probes), which detects the accumulation of a fluorescent oxidized product and can be used to calculate absolute H₂O₂ yield with appropriate standards. On top of washed NCI-H292 or NHBE cells on transwells, 50 μl HBSS was placed containing ionomycin (1 μM) or ATP (300 μM). Supernatants were collected at the end of a 20-min incubation and incubated in dark with an equal volume of HBSS containing 100 μM Amplex Red and 20 U/ml HRP. After 30 min, fluorescence was measured in a microplate reader (Fluoroskan Ascent) using excitation at 530 nm and emission at 590 nm. H₂O₂ release was quantified (fmol H₂O₂/20 min/mm²) using standard calibration curves. Both assays measured extracellular, not intracellular, H₂O₂, since omitting HRP from the reaction mix completely abolished the signals.

Measurement of superoxide production

Intracellular superoxide production was measured spectrophotometrically by the quantitative NBT reduction assay. Cells (10⁶/ml) were incubated in the presence of 1.3 mg/ml NBT for 30 min. Cells were centrifuged and washed twice in HBSS to remove extracellular formazan particles. Cells and intracellular formazan precipitates were dissolved in 2 M NaOH and DMSO, and the absorbance was measured at 720 nm in a microplate reader (VersaMax, Molecular Devices).

Extracellular superoxide production was measured by the Diogenes cellular luminescence enhancement system (National Diagnostics). Cells (10⁶/ml) were preincubated (10 min, 37°C) with or without 10 μM DPI on a 96-well (opaque white) plate (Thermo). An equal volume of Diogenes reagent containing stimuli was added, and luminescence was measured in a luminescence 96-well plate reader (Luminoskan Ascent). Data are expressed as int. RLU.

Measurement of changes in intracellular calcium concentration

Attached NCI-H292 cells were loaded with 4 μM fura 2-AM (Sigma-Aldrich) for 60 min in the dark. Loaded cells were trypsinized, washed, and placed into wells of black 96-well plates (Corning). After stimulation, changes in fluorescence were measured using 340 nm and 390 nm excitation wavelengths, with emission set at 510 nm. After the subtraction of the background of unloaded cells, the 340/390 ratio was determined.

Bacterial killing

The upper surfaces of NHBE cells differentiated on ALI transwells were washed, and fresh culture medium was placed in the bottom chamber. The cells were preincubated for 10 min with 2 μl of HBSS containing DPI, LPO, SCN⁻, catalase, ascorbic acid, cysteine, and Pyo (added to their exposed apical surface as indicated) before the addition of an additional volume of 3 μl of HBSS containing all the same components, plus the calcium mobilizing agonist (ATP or ionomycin) and 5,000 or 10,000 CFUs of *P. aeruginosa* or *B. cepacia*. Airway cells and bacteria were cocultured

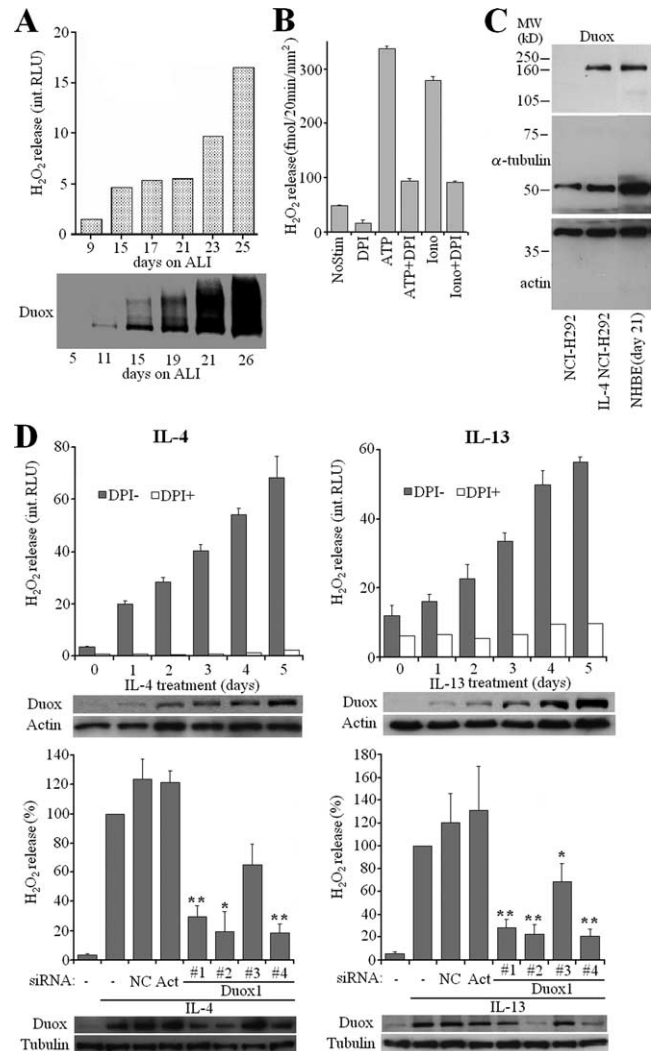
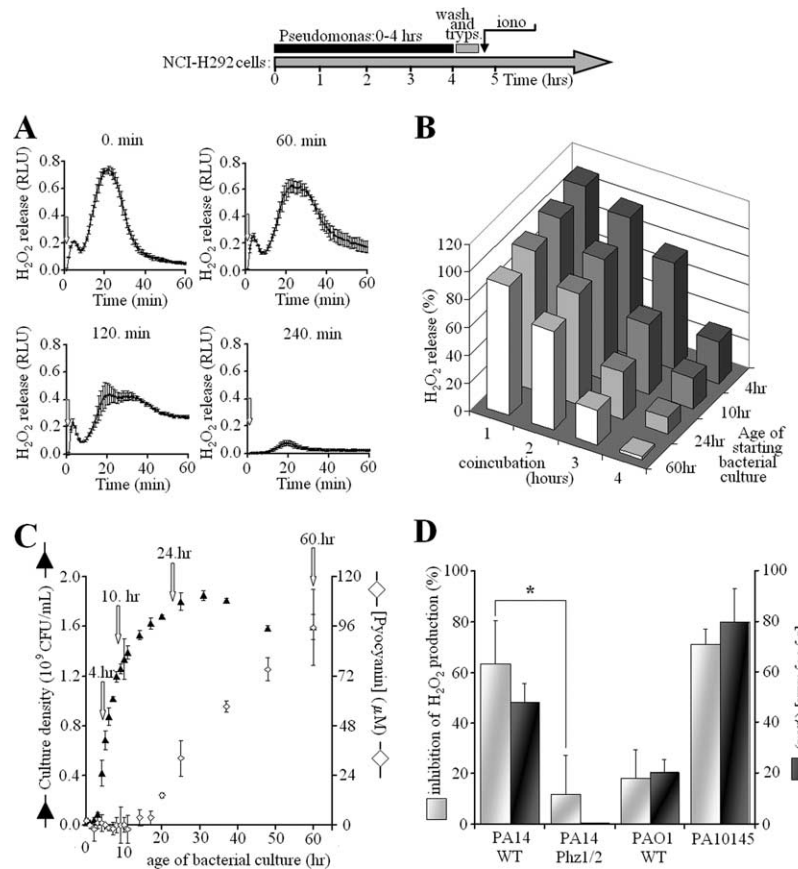


FIGURE 1. Duox-dependent H₂O₂ production by cytokine-induced NCI-H292 cells and NHBE cells. **A**, Ionomycin-triggered H₂O₂ release (luminol + HRP) and Duox protein levels were determined in NHBE cells cultured up to 26 days on ALI transwells. **B**, Quantified extracellular H₂O₂ release (Amplex Red + HRP) by attached NHBE cells (ALI day 21) using ionomycin (1 μM) or ATP (300 μM) as stimuli (mean ± SEM, n = 3). **C**, Duox levels were compared by Western blotting in noninduced and cytokine-induced (3 days) NCI-H292 cells and NHBE cells (21 days on ALI; one representative experiment, n = 2). **D**, upper panels, NCI-H292 cells were treated with 10 ng/ml IL-4 or IL-13 for 0–5 days and were assayed for H₂O₂ release by luminescence in the presence or absence of DPI (10 μM). Shown are results (means ± SD of triplicates) from one representative experiment of three. Inhibition of ionomycin-triggered H₂O₂ release by DPI (10 μM) in NCI-H292 cells after a 3-day induction by cytokines was: 88.2 ± 1.3% (IL-4, n = 39) and 80.0 ± 2.5% (IL-13, n = 12) (means ± SEM). Duox Western blotting during this time course is shown below. Lower panels, NCI-H292 cells were treated with negative control, actin (Act), or different Duox1-targeted siRNAs (Nos. 1–4). Cells were induced by 10 ng/ml IL-4 or IL-13 for 3 days, and Duox1 protein levels and ionomycin-triggered, DPI-sensitive H₂O₂ release (luminescence) were measured. Output is expressed as percentage of cytokine-induced H₂O₂ release detected in the absence of siRNAs (means ± SEM, n = 4 for both cytokines). Relative inhibition of the H₂O₂ output by the Duox1 siRNAs: IL-4, No. 1, 70.5%; No. 2, 80.3%; No. 3, 35.1%; No. 4, 81.5% (mean, n = 4); IL-13, No. 1, 71.9%; No. 2, 77.5%; No. 3, 31.1%; No. 4, 79.1% (mean, n = 4). Significance levels are compared with negative control (NC).

FIGURE 2. Exposure of airway cells to *P. aeruginosa* inhibits Duox activation. As shown on the scheme, attached, IL-4-induced NCI-H292 cells were coincubated with *P. aeruginosa* for 0–4 h. Bacteria grown for 4–60 h were washed and resuspended in RPMI 1640 and exposed to airway epithelial cells (multiplicity of infection of 10:1). After that, bacteria were removed and NCI-H292 cells were washed (PBS), trypsinized, and assayed for DPI-sensitive, ionomycin (iono)-triggered H_2O_2 release (luminol + HRP). **A**, Ionomycin-stimulated H_2O_2 release by IL-4-induced NCI-H292 cells is inhibited by prior exposure to *P. aeruginosa* (strain PA10145) for different times (0, 60, 120, 240 min). Kinetic data represent means \pm SD of triplicates from one representative experiment out of three. **B**, Ionomycin-stimulated, DPI-sensitive H_2O_2 release by IL-4-induced NCI-H292 cells was compared as a function of exposure time to PA10145 (bottom axis) and age of PA10145 culture added to cells (right axis). **C**, Biosynthesis of Pyo in long-term cultures of PA10145 detected by OD of supernatants (A_{691} , \diamond). Bacterial culture densities were monitored by A_{600} (\blacktriangle) and converted into concentration of CFUs ($OD = 1.0$ corresponds to 10^9 CFUs/ml). Arrows denote times at different growth phases: 4 h (early), 10 h (late exponential), 24 h (early stationary), 60 h (late stationary). **D**, Duox inhibition by *P. aeruginosa* strains (PA10145, PA14WT, PA14 Phz1/2, and PAO1) correlates with their Pyo production (means \pm SEM, $n = 3$). Bacteria were previously grown for 60 h and then added to NCI-H292 cells for 4 h. *, $p < 0.05$ for Phz1/2 compared with WT PA14.



for 3 h (37°C) before lysing cells in 1 ml HBSS containing 1 mg/ml saponin. One to 10 serial dilutions were spread on LB agar plates in triplicate. Colonies were counted the next day to calculate bacterial killing efficiencies.

In vitro oxidation of Pyo by peroxidases

The *in vitro* oxidation of Pyo by peroxidases was monitored in a 96-well microplate spectrophotometer (VersaMax) by measuring decreases in the concentration of the unoxidized, unprotonated form at its absorption maximum at 691 nm, based on a standard calibration curve (see Fig. 7E). The data shown as “conversion of Pyo” in Fig. 7, C and D, reflect decreases in the concentration of the unprotonated, unoxidized form of pyocyanin with time. The reactions were conducted at 37°C in solutions supplemented with LPO, MPO, H_2O_2 , and Pyo (at concentrations indicated in the Fig. 7 legend), but lacking chloride. The pH was maintained above 6.0 to avoid absorbance changes (691 nm) related to Pyo acidification.

Statistical analysis

Data are represented either as means \pm SEM of at least three independent experiments or as means \pm SD of one representative experiment out of at least two similar independent ones. Significance levels were compared using Student's *t* test: *, $p < 0.05$; **, $p < 0.01$; ***, $p < 0.001$.

Results

Duox is induced in differentiated primary human bronchial epithelial cells cultured on ALI and in NCI-H292 cells treated with Th2 cytokines IL-4 and IL-13

To study possible interactions of Duox and Pyo, we used two different airway epithelial models: primary NHBE cells and a human mucoepidermoid pulmonary carcinoma cell line that also produces Duox, NCI-H292. Low-passage NHBE cells were grown on transwells on ALI to mimic the airway environment and promote a mature cellular phenotype (23). After seeding NHBE cells on ALI, they develop into polarized, terminally differentiated cells

during the course of 2–3 wk, showing characteristic markers of mature airway epithelium (mucin expression, ciliogenesis). During this differentiation process, Duox expression and H_2O_2 release also increased gradually (Fig. 1A). H_2O_2 release was triggered by Ca^{2+} -mobilizing agonists (ATP, ionomycin) and was inhibited by the flavoenzyme inhibitor DPI (Fig. 1B). Since Duox1 induction was demonstrated in NHBE cells by Th2 cytokines IL-4 and IL-13 (28), we examined the effects of these cytokines on Duox levels in NCI-H292 cells. These cytokines also induce Duox in NCI-H292 cells after 3-day treatments at levels comparable with primary cells grown on ALI for 21 days (Fig. 1C), although the induced NCI-H292 cells produced significantly lower amounts of H_2O_2 . The IL-4-induced NCI-H292 cells produced $5.69 \text{ pmol } H_2O_2/\text{min}/10^6 \text{ cells}$ in response to ionomycin when measured on cell suspensions prepared at high cell concentrations (mean, $n = 2$, Amplex Red/HRP). The same assay was not sensitive enough to detect H_2O_2 released from cells (IL-4 NCI-H292) when attached to transwells, because of the much lower amount of cells obtained under this condition. In contrast, ALI NHBE cells on transwells produced $247.3 \pm 5.45 \text{ fmol}/20 \text{ min}/\text{mm}^2 H_2O_2$ (average \pm SEM, $n = 3$; DPI-sensitive) in response to ATP (or similar amounts by ionomycin), indicating that the differentiated primary cells have a much higher H_2O_2 output than do cytokine-induced NCI-H292 cells. This higher H_2O_2 output explains functional differences in microbial killing capabilities of the two cell types (see below).

IL-4 and IL-13 induced higher Duox levels steadily during the course of 5 days (Fig. 1D), whereas induction of Duox2 by the Th1 cytokine IFN- γ was less consistent (data not shown). Parallel with induction of Duox, DPI-sensitive H_2O_2 release by NCI-H292 cells increased following IL-4 or IL-13 treatments (Fig. 1D). Interestingly, both cytokines are detected at higher than normal levels in

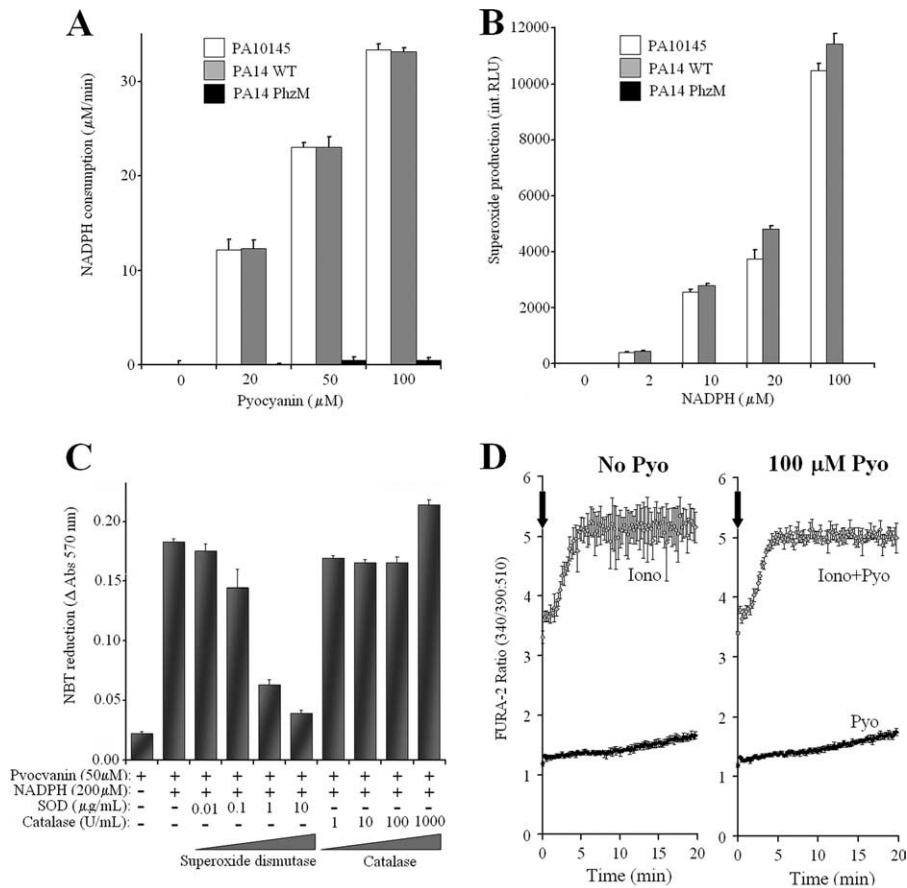


FIGURE 3. Characterization of purified Pyo. *A*, Purified Pyo consumes NADPH in vitro. Supernatants of 2.5-day-old cultures of *P. aeruginosa* WT (PA14 and PA10145) and Pyo-deficient mutant (PA14 PhzM) strains were processed in parallel to extract Pyo, as described in *Materials and Methods*. Purified Pyo, or equivalent volumes of the extracts from the mutant strain, were incubated in vitro with 1 mM NADPH for 20 min. NADPH consumption was measured by following the changes in absorbance at 340 nm and calibrated using samples with known NADPH concentrations. One representative result (mean \pm SD of triplicates) of three independent experiments is shown. *B*, Purified Pyo generates superoxide from NADPH. Pyo (50 μ M) or equivalent mutant extracts were incubated in vitro with NADPH in HBSS, and superoxide production was measured by Diogenes chemiluminescence (20 min). One representative result (mean integral luminescence \pm SD of triplicate assays) of three independent experiments is shown. *C*, Pyo reduces NBT in vitro through generation of superoxide. Pyo, NADPH, and superoxide dismutase (SOD) or catalase were incubated in vitro for 60 min in the presence of NBT, and absorbance changes at 570 nm were measured. Results are means \pm SD of triplicates of one experiment out of two. *D*, Pyo does not affect calcium signaling in NCI H292 cells. The fura 2-AM-loaded, IL-4-induced NCI-H292 cells were stimulated by ionomycin (1 μ M), Pyo (100 μ M), both of them, or none of them. Changes in the ratio of fura 2-AM fluorescence were followed for 20 min. Data are means \pm SD of quadruplicates of one representative experiment. In four separate experiments the increases in fura 2-AM ratios during the 20 min time were: unstimulated, 0.49 ± 0.057 ; Pyo, 0.43 ± 0.047 ; ionomycin, 3.03 ± 0.44 ; ionomycin + Pyo, 3.16 ± 0.52 (mean \pm SEM, $n = 4$). Differences between the Pyo-free vs Pyo-containing values were not significant.

bronchial lavage from CF patients (29). Both Duox protein levels and H_2O_2 release were diminished by Duox1-targeted siRNA-treatment. Three Duox1 siRNAs (Nos. 1, 2, and 4) out of four tested decreased DPI-sensitive H_2O_2 release by >70% (Fig. 1*D*, lower panels). The results show that Duox1 is the principal source of Ca^{2+} -dependent extracellular H_2O_2 release by NCI-H292 cells and that these cells are a suitable model to study expression and function of this airway oxidase.

Prolonged exposure to WT *P. aeruginosa* PA10145 inhibits Duox-mediated H_2O_2 production

To study the influence of *Pseudomonas* on Duox-mediated H_2O_2 release, we incubated attached, cytokine-induced NCI-H292 cells with *P. aeruginosa* bacteria for up to 4 h, and then the bacteria were washed away and the NCI-H292 cells were stimulated by the Ca^{2+} ionophore ionomycin. We found that prolonged exposure of IL-4-induced NCI-H292 cells to WT PA10145 blocked Duox-mediated H_2O_2 release in response to ionomycin (Fig. 2*A*). H_2O_2

release decreased with increased bacterial exposure and was entirely abolished after 240 min of exposure to bacteria from overgrown (60 h) cultures (Fig. 2, *A* and *B*). During the 4-h incubation, Duox protein levels did not change, nor was there evidence of degradation as judged by Western blotting (data not shown). This inhibitory effect of coincubation of bacteria with airway cells was diminished when exposed to fresh *P. aeruginosa* cultures, suggesting that the bacteria produce some Duox inhibitory component in long-term culture (Fig. 2*B*). *P. aeruginosa* has a complex life cycle, starting with planktonic cells that seed microcolonies and then form macrocolonies, which leads to establishment of biofilms. This can be mimicked in overgrown suspension cultures. One indication of these changes is the production of a blue-green pigment, Pyo, which appears as a consequence of quorum sensing in late phases of cultivation (Fig. 2*C*). Pyo is a good candidate for Duox inhibition, since it is secreted, cell permeable, and a redox-active compound capable of consuming intracellular NADPH.

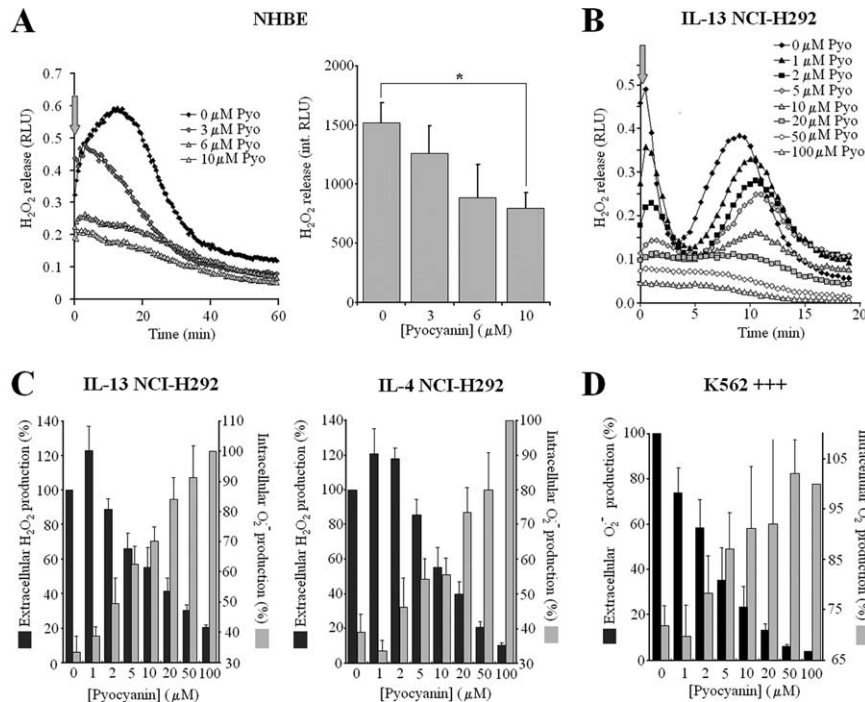


FIGURE 4. Effects of purified Pyo on Duox activity in airway epithelial cells. **A**, Ionomycin-stimulated H_2O_2 release by adherent NHBE cells (ALI, day 21) is inhibited by Pyo (30-min pretreatments). *Left panel*, Kinetics of one representative experiment (mean of duplicates) out of four. *Right panel*, Averaged data (integrated RLU over 60-min assays) of the four experiments, with each performed in triplicate (luminol + HRP; mean \pm SEM). **B**, Representative kinetics of H_2O_2 release by IL-13-induced NCI-H292 cells when ionomycin ($1 \mu\text{M}$) and Pyo (0–100 μM) were added together. Each curve represents the mean of triplicate assays of one representative experiment; five others gave similar results. **C**, Pyo inhibits extracellular H_2O_2 release (black bars) while producing intracellular O_2^- (gray bars). IL-4- and IL-13-induced NCI-H292 cells were stimulated by ionomycin ($1 \mu\text{M}$) and Pyo (0–100 μM) together, and both extracellular H_2O_2 release (luminol + HRP; mean \pm SEM of total integrated 20-min output, normalized to Pyo-free cells; IL-4, $n = 8$, IL-13, $n = 6$; all experiments were performed in triplicate) and intracellular O_2^- production (20-min NBT reduction; mean \pm SEM normalized to values obtained with 100 μM Pyo for both cytokines; $n = 3$) were measured. **D**, K562 $^{+++}$ cells were stimulated by 100 nM PMA together with different concentrations of Pyo (0–100 μM). Shown are intracellular (NBT reduction, mean \pm SEM normalized to the Pyo-free cells, $n = 3$) and extracellular (integrated Diogenes luminescence; mean \pm SEM normalized to 100 μM Pyo-treated cells, $n = 4$) superoxide production over 20-min time courses.

Duox inhibition by *P. aeruginosa* WT strains correlates with their Pyo-producing capabilities

In addition to the PA10145 WT strain, we compared two other WT strains that produce Pyo at different rates. Average Pyo concentrations in 2.5-day-old cultures were: 55.5 μM (*P. aeruginosa* 14 WT (PA14 WT)), 21.2 μM (*P. aeruginosa* PAO1 WT (PAO1 WT)), and 92.3 μM (PA10145) (average, $n = 4$) (Fig. 2D). Pyo appeared rapidly in the medium of PA14 WT and reached peak concentrations at 24–36 h, whereas PA10145 was a slow producer but reached higher final concentrations. When 2.5-day-old cultures of each WT strain were coincubated with attached IL-4 NCI-H292 cells for 4 h (multiplicity of infection of 10:1) and ionomycin-triggered H_2O_2 release was determined, the extent of Duox inhibition correlated with the Pyo producing capabilities of the WT strains (Fig. 2D). The fact that the pronounced inhibition of Duox activity by the WT PA14 strain disappeared when its phenazine-deficient mutant, Phz1/2, was used strongly suggested Pyo is the cause of Duox inhibition (Fig. 2D).

Duox activity is inhibited by Pyo

To confirm this relationship of Pyo production and Duox inhibition, we purified Pyo from supernatants of the two best WT producers (PA14 WT and PA10145). Pyo purified from both strains consumed NADPH (Fig. 3A) and produced O_2^- (Fig. 3, B and C) in vitro, while comparable extracts from the *P. aeruginosa* Phz1 mutant had no activity. Fig. 3C shows that the primary product of

Pyo-mediated reduction of oxygen is superoxide, not H_2O_2 . Purified Pyo by itself did not induce any calcium signals in fura 2-AM-loaded NCI-H292 (IL-4-induced) cells nor did it interfere with ionomycin-triggered increases in intracellular calcium concentrations (Fig. 3D).

We then studied the effects of the purified toxin on Duox activity in different cell types. NHBE cells grown on transwell ALI cultures were washed, treated on their apical surface with Pyo (30 min; 3, 6, and 10 μM), and washed again before measuring ionomycin-induced H_2O_2 release. Pretreatment of NHBE cells with purified toxin inhibited Duox activity in a concentration-dependent manner, showing 50% inhibition at 10 μM Pyo (Fig. 4A).

To test the possibility that Pyo entering cells and Duox compete for NADPH, we added Duox activator (Ca^{2+} ionophore) and the toxin together to cytokine-treated NCI-H292 cells and measured extracellular H_2O_2 release in parallel with intracellular O_2^- production (Duox produces extracellular H_2O_2 , whereas Pyo forms intracellular O_2^- from the same intracellular pool of NADPH). Extracellular H_2O_2 release was inhibited in a dose-dependent manner by Pyo in both IL-13-induced (Fig. 4, B and C) and IL-4-induced (Fig. 4C) NCI-H292 cells. Intracellular O_2^- production was directly proportional to toxin concentrations and inversely proportional to extracellular H_2O_2 detected (Fig. 4C). The toxin-derived superoxide was detectable as extracellular H_2O_2 release as well in NCI-H292 cells not stimulated by ionomycin, but these levels were much

lower than those observed when Duox was activated (data not shown). Thus, Pyo inhibits Duox activity as it “transforms” extracellular H_2O_2 release aimed at destroying bacteria into intracellular O_2^- , thereby exposing the cell interior to oxidative attack. We confirmed that NBT reduction by Pyo and NADPH occurs predominantly through O_2^- generation and not through direct reduction under aerobic conditions, since it was inhibited by superoxide dismutase in vitro (Fig. 3C). Furthermore, Pyo did not interfere with the luminol plus HRP H_2O_2 detection system, as it was shown by using glucose plus glucose oxidase as an alternative H_2O_2 source, which produced luminescence independent of Pyo concentrations (data not shown).

This inhibitory mechanism of Pyo could also apply to other Nox family members, since they all consume NADPH while reducing molecular oxygen into O_2^- within an extracytoplasmic compartment. Pyo has been shown to inhibit the respiratory burst of PMA-stimulated human neutrophils (30). We confirmed these observations (data not shown). Furthermore, we used K-562 cells reconstituted with the complete Nox2 system (K562⁺⁺⁺ cells) and showed that Pyo inhibited extracellular O_2^- production in a dose-dependent manner, while producing intracellular O_2^- (Fig. 4D).

Pyo blocks cytokine-induced Duox up-regulation in airway epithelial cells

We tested whether Pyo also affects Duox protein levels following long-term treatment of airway epithelial cells by cytokines. When IL-4 or IL-13 was added together with Pyo to confluent NCI-H292 cells for 3 days, complete inhibition of Duox up-regulation was observed, which correlated with diminished H_2O_2 release (Fig. 5A) (inhibition by 8 μ M Pyo was $85.0 \pm 2.9\%$ (mean \pm SEM, $n = 39$)). When the most potent inhibitory concentration of Pyo (8 μ M) used on NCI-H292 cells was applied to primary NHBE cells, the toxin blocked Duox induction by all three cytokines, that is, IL-4, IL-13, and IFN- γ (Fig. 5B). To confirm these observations, we subjected supernatants of PA14 WT, pyo-deficient PhzM and bacterium-free LB medium to the Pyo extraction and purification protocol and processed them in parallel. When Pyo or the equivalent volume of the PhzM or LB extract was added together with IL-4 to NCI-H292 cells, only the WT extract containing Pyo had an inhibitory effect on H_2O_2 release and Duox protein levels, whereas the two other preparations were without effect (Fig. 5C). This confirms that Pyo, and not some other residual bacterial components in the Pyo preparation, is responsible for the observed inhibition. Since oxidative stress is considered to be the cause of most of the toxic effects of Pyo, we examined whether reactive oxygen species (ROS) scavengers had an effect on the Pyo-mediated inhibition of Duox up-regulation in IL-4-induced NCI-H292 cells. *N*-acetylcysteine (NAC) at concentrations of 10 mM prevented partially the inhibition of H_2O_2 release and corresponding decreases in Duox protein levels, whereas 5 mM glutathione (GSH) prevented such inhibition completely (Fig. 5D).

Pyo inhibits killing of *P. aeruginosa* by the Duox/LPO/SCN⁻ system on airway cells

Next, our aim was to test the presence of Pyo on the ultimate function of the H_2O_2 /LPO/SCN⁻ system, namely microbial killing. First, we confirmed that bacterial killing by primary NHBE cells is Duox dependent (18). Survival of *Pseudomonas* was unchanged when one or more components of the H_2O_2 /LPO/SCN⁻ system were omitted, and killing occurred only when the entire system was present (Fig. 6A). Inhibition of Duox by DPI, scavenging of H_2O_2 by catalase or ascorbic acid, or omission of ATP as a stimulus of H_2O_2 release prevented *Pseudomonas* killing (Fig.

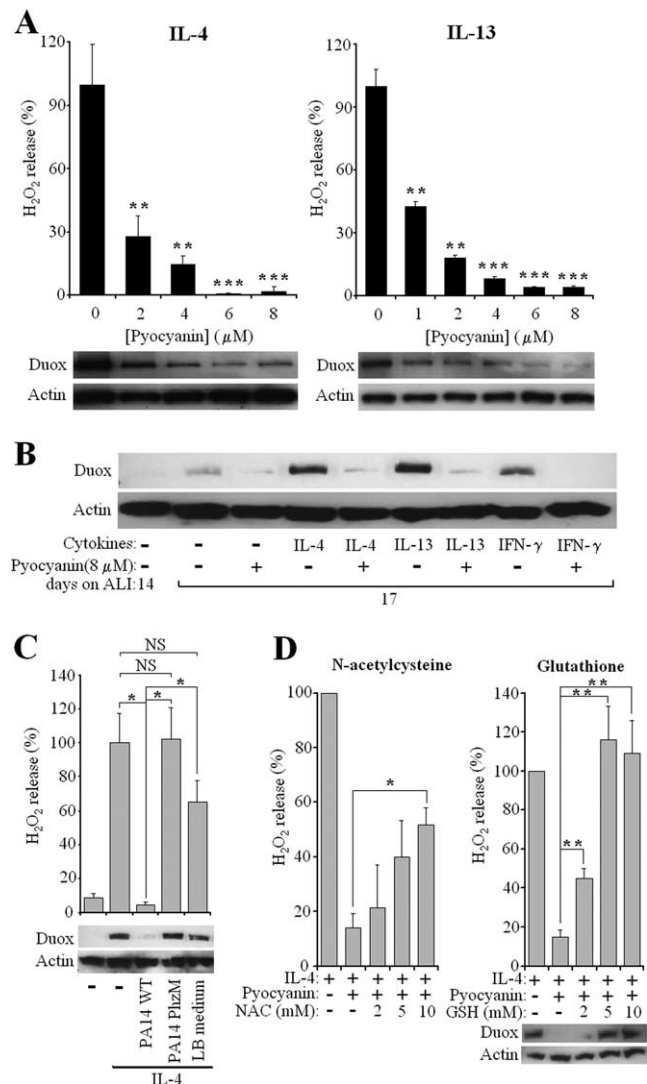


FIGURE 5. Pyo blocks up-regulation of Duox by cytokines. **A**, NCI-H292 cells were incubated 3 days with cytokines (IL-4 or IL-13) and Pyo (0–8 μ M). Duox protein levels and ionomycin-triggered H_2O_2 release (DPI-sensitive) were measured relative to Pyo-free cells (means \pm SEM, $n = 4$). Significance levels are from comparisons with cells not treated with Pyo. **B**, Fourteen-day-old NHBE cells were induced, or not, by three cytokines (IL-4, IL-13, and IFN- γ) with or without 8 μ M Pyo. Cells were Western blotted 3 days later for Duox protein levels. Similar results were observed using cells from three different donors. **C**, NCI-H292 cells were treated together with IL-4 and 8 μ M Pyo prepared from the supernatant of PA14 WT strain or equivalent extract from PhzM mutant or LB medium by itself. After 3 days of induction, NCI-H292 cells were assayed for DPI-sensitive, ionomycin-stimulated H_2O_2 release (luminol +HRP) and Duox protein levels. Shown are the results (percentage of Pyo-free cells) of three experiments each performed in triplicate (means \pm SEM). **D**, ROS scavengers permit Duox induction in the presence of Pyo. NCI-H292 cells were treated with IL-4 and 8 μ M Pyo \pm ROS scavengers (NAC and GSH) for 3 days. Cells were assayed for ionomycin-stimulated H_2O_2 release and for Duox levels. Data are shown as percentage of values of cells treated only by IL-4 (means \pm SEM, $n = 4$ (GSH), $n = 3$ (NAC)).

6A). We also showed that the system is lethal against another airway pathogen, *B. cepacia* (Fig. 6A); in this case, H_2O_2 release was triggered by ionomycin. Addition of the ROS scavenger cysteine inhibited killing of *B. cepacia* (Fig. 6A). To investigate the effect of Pyo on killing, NHBE cells were preincubated with 2, 10, or 20 μ M Pyo for 10 min, and then 5000 CFU of PA10145 were added

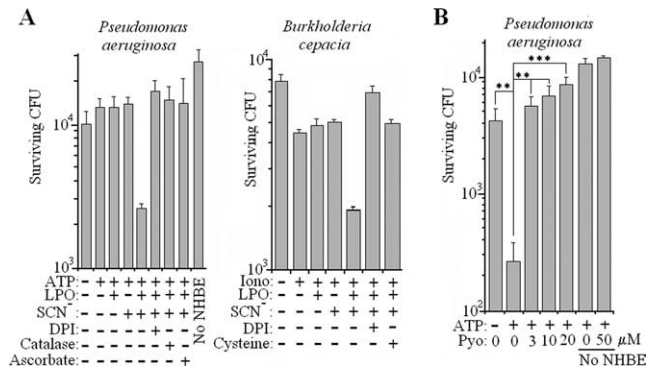


FIGURE 6. Pyo inhibits microbicidal activity of the Duox/LPO/SCN⁻ system on primary human airway cells. *A*, Three-week-old ALI cultures of NHBE cells were exposed for 3 h to 10,000 CFU of *P. aeruginosa* PA10145 or 5,000 CFU of *B. cepacia* in the presence of different components or inhibitors of the Duox/LPO/SCN system, as indicated. Bacterial survival was measured by plating and colony counting. Data are means \pm SD (quadruplicates) of one representative experiment out of two; Iono indicates ionomycin. *B*, Three-week-old NHBE cells were first incubated for 10 min with Pyo, and then *P. aeruginosa* microbicidal assays were performed as in *A*. Data present means \pm SD (quadruplicates) of one representative experiment out of two.

together with LPO, SCN⁻, and ATP. When Duox was activated by ATP, survival of PA10145 decreased dramatically, showing a potent microbicidal effect of the Duox/LPO/SCN⁻ system (Fig. 6*B*). Pretreatment of airway cells with Pyo blocked the killing of *Pseudomonas* (Fig. 6*B*). Pyo had no direct effect on the survival of the bacteria (Fig. 6*B*). These data show that Pyo is a potent virulence factor of *P. aeruginosa* capable of suppressing bacterial killing by the Duox/LPO/SCN⁻ system.

LPO and myeloperoxidase (MPO) oxidize Pyo using H₂O₂

In addition to LPO, appreciable levels of MPO are also found in the airway surface liquid. MPO is released from neutrophil granulocytes that migrate to the inner surface of airways. Both enzymes use H₂O₂ to oxidize a broad range of compounds, and earlier studies have shown that MPO can oxidize several bacterial toxins: pneumolysin from *Streptococcus pneumoniae*, leukotoxin from *Actinobacillus actinomycetemcomitans* (31), and *Clostridium difficile* cytotoxin (32). Previous studies showed that Pyo is oxidized by hemin or microperoxidase, a degradation product of cytochrome *c* (21).

Herein, we show that both LPO and MPO can oxidize Pyo and convert it into a less toxic derivative. Neither LPO nor H₂O₂ alone decreased detectable Pyo levels, but when added together Pyo concentrations dropped (Fig. 7*A*). Similar results were obtained with MPO (Fig. 7*B*). Consumption of Pyo by LPO is dependent on the concentrations of LPO (Fig. 7*C*) and H₂O₂ (Fig. 7*D*). When Pyo is incubated with LPO and H₂O₂ together, the absorption spectrum of Pyo changes, with diminished absorbance peaks at 279 and 691 nm, reflecting the disappearance of the original form of the toxin (Fig. 7*E*). To show that conversion of Pyo by LPO and MPO renders it less toxic, we incubated 30 μ M Pyo in the presence or absence of H₂O₂ and different concentrations of LPO and MPO. At the end of overnight incubations, each solution was added to NCI-H292 cells suspended in HBSS containing nitro blue tetrazolium to measure intracellular O₂⁻ production. The presence of H₂O₂, LPO, or MPO alone did not decrease Pyo-mediated, intracellular O₂⁻ production, but addition of the peroxidases together with H₂O₂ decreased the intracellular toxicity of Pyo (O₂⁻ formation) in a dose-dependent manner (Fig. 7*F*). Thus, both LPO and MPO can protect

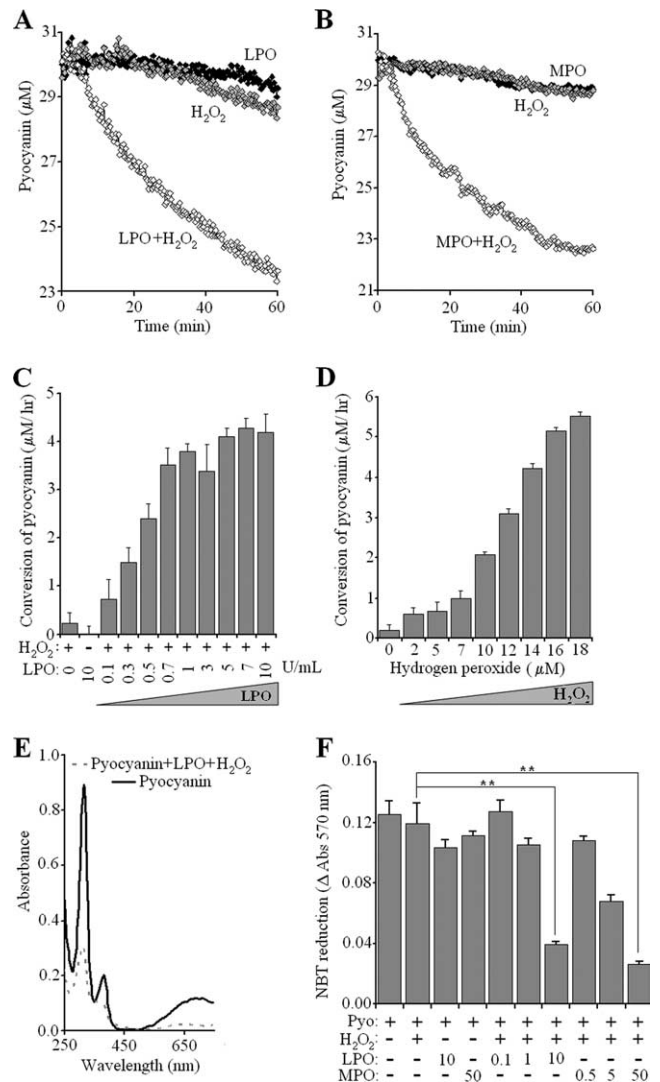


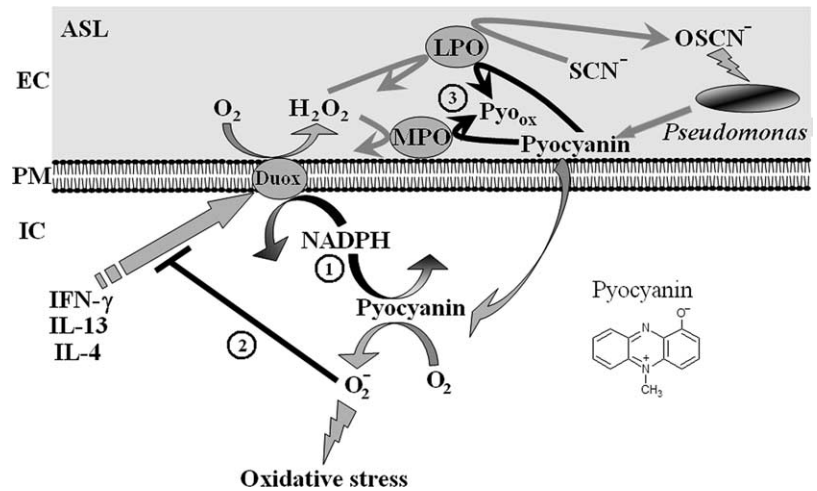
FIGURE 7. Peroxidase-mediated detoxification of Pyo. Changes in Pyo (initially 30 μ M) were followed spectrophotometrically in the presence of 100 μ M H₂O₂ and 10 U/ml (3.47 μ M) LPO (*A*) or 50 μ g/ml (335 nM) MPO (*B*). Shown is one representative result of three. *C*, Pyo consumption (μ M/h) in the presence of 200 μ M H₂O₂ and LPO (mean \pm SEM, *n* = 4). *D*, Pyo consumption (μ M/h) in the presence 5 U/ml (1.74 μ M) LPO and H₂O₂ (mean \pm SEM, *n* = 4). *E*, Absorption spectra of Pyo after overnight incubation in the presence or absence of 100 μ M H₂O₂ and 20 U/ml LPO. *F*, After overnight incubation (37°C) of solutions containing Pyo (30 μ M), H₂O₂ (100 μ M), LPO (0.1, 1.0, 10 U/ml), or MPO (0.5, 5.0, 50 μ g/ml), 5 μ l was added to trypsinized and washed NCI-H292 cells (10⁶/ml, 650 μ g/ml NBT), incubated for 30 min, and then intracellular O₂⁻ production was determined (mean \pm SEM, *n* = 3).

human airway epithelial cells from the oxidative stress imposed by Pyo exposure.

Discussion

CF is an autosomal recessive genetic disorder that affects ~1 in 2500 individuals, mainly of Caucasian origin. The primary cause is mutations in the CFTR chloride channel, but how these genetic defects manifest in lung disease characterized by frequent and chronic bacterial infections remains a debated issue (33, 34). Models citing the reduced volume and increased viscosity (dehydration) of CF ASL that can impede ciliary clearance of airway pathogens are inadequate in explaining the unique susceptibility of CF patients to particular airway pathogens. Human mucosal surfaces

FIGURE 8. Multiple redox-based interactions involving Pyo and the human airway Duox/LPO/SCN⁻ system. Duox-derived H₂O₂ supports LPO-mediated conversion of thiocyanate (SCN⁻) into hypothiocyanite (OSCN⁻), which is effective against oxidant-sensitive pathogens (several species that infect CF lungs). Pyo is a membrane-permeable microbial metabolite that enters cells and reacts with intracellular NADPH (1). Diminished NADPH levels support lower Duox activity, thereby enhancing bacterial survival. Reduced Pyo reacts with oxygen and produces intracellular O₂⁻ (oxidative stress), which inhibits cytokine induction of Duox (2) and limits H₂O₂ release. Duox-derived H₂O₂ and airway peroxidases can oxidize Pyo (Pyo_{ox}), thereby decreasing its cytotoxicity (3).



are equipped with numerous antimicrobial systems. Among them, LPO and its substrate thiocyanate are well recognized as abundant, effective antimicrobial components of several exocrine secretions (milk, tears, saliva), although only recently has this system been appreciated within the ASL. Our laboratory suggested Duox1 and Duox2 serve as mucosal sources of H₂O₂ capable of supporting LPO activity in the generation of the microbicidal oxidant hypothiocyanite (12, 35). Later studies confirmed our observations that detected Duox1 as the predominant oxidase in human major airway epithelial cells, showed that Duox1 is induced by Th2 cytokines IL-4 and IL-13 (28), and proposed other defense-related functions for Duox1, including acid (36) and mucin secretion (37). We suggested that the immunocompromised phenotype in CF may reflect microbial killing defects by the airway Duox/LPO/SCN⁻ system by noting that organisms typically infecting CF airways in early disease stages (i.e., *S. aureus*, *B. cepacia*) also commonly infect chronic granulomatous disease patients who suffer from defects in oxidative killing in phagocytes (12). Furthermore, we hypothesized that impaired performance of the Duox/LPO/SCN⁻ antimicrobial system could stem from CFTR gene defects, since this channel is known to exhibit efficient SCN⁻ transport activity (9). Two recent studies explored the model in more detail, showing that the impaired SCN⁻ transport activity of human CF airway epithelial cells is sufficient to compromise LPO- or ROS-dependent microbial killing in vitro (18, 38). Our current observations, together with these studies, indicate that the human airway Duox1/LPO/SCN⁻ system is indeed capable of killing several pathogens that frequently infect the lungs of CF patients, including *P. aeruginosa*, *S. aureus*, *B. cepacia*, and *H. influenzae*. Further study is needed to confirm the consequences of CFTR mutations on the Duox/LPO/SCN⁻ antimicrobial system in CF lungs and consider the effectiveness of supplemental SCN⁻ inhalation therapy in these patients.

Although the host factors that predispose CF patients to *P. aeruginosa* colonization are unclear, it is known that inducible microbial virulence factors have important roles in CF disease pathogenesis following the establishment of chronic infections. The importance of antimicrobial systems can become evident when targeted by microbial virulence factors. Production of Pyo and other virulence factors is turned on through microbial quorum sensing during advanced stages of chronic *P. aeruginosa* infection, usually coinciding with appearance of the mucoid phenotype and biofilm formation. Pyo is produced in most *P. aeruginosa* clinical isolates from patients suffering from diverse lung diseases and is detected in high concentrations in *P. aeruginosa*-infected patients with bronchiectasis and CF (39). Studies on a variety of other *P.*

aeruginosa-infected organisms showed that Pyo-deficient mutant strains are markedly less capable of killing their hosts, including *C. elegans*, plants, *Drosophila*, and mice (21). Our studies show that physiologically relevant Pyo concentrations interfere with the Duox/LPO/SCN⁻ antimicrobial system on at least two levels: 1) Pyo enters airway cells, oxidizes NADPH, and produces O₂⁻, thereby inhibiting the extracellular production of H₂O₂ by Duox while imposing intracellular oxidative stress (Fig. 8, process 1); and 2) over the long term, Pyo also blocks cytokine induction of Duox1, such that the host is unable to respond to bacterial challenge with enhanced H₂O₂ release (Fig. 8, process 2). Thus, this pathogen targets the Duox/LPO/SCN⁻ system and by inhibiting it may improve survival of this and other bacterial species in the human respiratory tract. We show that the Duox/SCN⁻/LPO system is also able to kill *B. cepacia*. Although less common than *P. aeruginosa* infection, *B. cepacia* infection carries the worst prognosis for CF (40). In many cases, *B. cepacia* and *P. aeruginosa* coinfest CF patients (41); under these conditions, Pyo produced with chronic *P. aeruginosa* infection could compromise *B. cepacia* killing by the host Duox/SCN⁻/LPO system. In other cases, organisms may be directly susceptible to redox-based toxicity of Pyo, which may explain the predominance of *P. aeruginosa* in late stages of CF disease.

Airway oxidative stress is another feature of the enhanced inflammatory state of CF airways in advanced disease. GSH levels are typically lower in CF ASL. We observed protective effects of GSH on Pyo-mediated inhibition of IL-4-induced Duox1 expression, raising the possibility that Duox protein levels in CF airway epithelium can be lower, leading to less efficient microbial killing by the H₂O₂/LPO/SCN⁻ system. The protective effects of GSH and the GSH precursor NAC on Duox activity or expression may explain the improvement of lung function in CF following administration of either of the two drugs. How Pyo blocks Duox induction by these cytokines and how GSH and NAC prevent this inhibition will require further study, although it is known that Pyo can oxidize GSH directly (42). Pyo could alter transcription of Duox and other ROS responsive genes or interfere with Duox protein folding or transport.

Our observations on the effects of Pyo on airway Duox activity may be generalized to include NADPH oxidases in other cell types. Excessive neutrophil infiltration is another hallmark of chronically infected CF lungs. We confirmed earlier observations showing that O₂⁻ production by neutrophils is inhibited by Pyo (30). Our observations in Nox2-reconstituted cells suggest that

competition for common substrates (NADPH and oxygen) between Pyo and the Nox2-based phagocytic oxidase is the mechanism for inhibition in these cells as well.

In one final aspect of this redox-based interplay between airway epithelium and pathogen, we show that two airway peroxidases, LPO and MPO, are also capable of oxidizing Pyo into less toxic species no longer capable of exerting redox-based effects on the host (Fig. 8, process 3). Here, we showed that Pyo is detoxified by H₂O₂ and physiological levels of LPO or MPO and that oxidized Pyo is less capable than untreated Pyo in inflicting intracellular oxidative stress on NCI-H292 airway cells. Similar observations were described in the detoxification of Pyo by microperoxidase 11, a peptide fragment of cytochrome *c* bound to heme, as reflected in diminished Pyo-induced IL-8 release by A549 cells (22). These findings suggest a new role for airway peroxidases and Duox in the ASL in detoxifying this virulence factor, but imply that Pyo can also prevent its own detoxification by inhibiting Duox when produced in excess by established biofilms. The results suggest augmentation of LPO-mediated Pyo oxidation in situ as a potential therapy for chronic *P. aeruginosa* infection.

In summary, our studies illustrate a complex network of redox-based interactions between human airway epithelial cells and *P. aeruginosa*, an opportunistic pathogen. Many of the reasons for its success in infecting immunocompromised individuals are not well understood, but the broad range of its virulence factors, its capability for biofilm formation, its resistance to many host defense mechanisms, and its adaptability to changing environments certainly contribute. Our data show that the human airway epithelium is equipped with potent oxidant-based defense mechanisms that are effective against airway pathogens and that *P. aeruginosa* can adapt to this environment with redox-based counteroffensive mechanisms. The novel findings in the battle between *P. aeruginosa* and the airway epithelium presented herein may help understand the pathogenesis of this microorganism.

Acknowledgments

This paper is dedicated to Dr. Bruno Reiter, a pioneer of the lactoperoxidase field who has provided invaluable advice and encouragement. The authors thank Carl Hammer (Mass Spectrometry Unit, National Institute of Allergy and Infectious Diseases, National Institutes of Health) for performing mass spectrometry analysis on Pyo preparations. We are also grateful for research materials from the following sources: The Pseudomonas Mutant Library (Manoil Laboratory, University of Washington, Seattle) for providing the PAO1 WT strain; Dr. Frederick M. Ausubel (Harvard University, Boston, MA) for sending us the PA14 WT and PhzM strains; Dr. You-Hee Cho (Sogang University, Seoul, South Korea) for providing the PA14 Phz1/2 strain; and Dr. Steven M. Holland (Laboratory of Clinical Infectious Diseases, National Institute of Allergy and Infectious Diseases, National Institutes of Health) for the clinical isolate of *B. cepacia*. We thank Dr. Miklós Geiszt (Semmelweis University, Budapest, Hungary) for many helpful discussions.

Disclosures

The authors have no financial conflicts of interest.

References

1. Reiter, B., and J. P. Perraudin. 1991. Lactoperoxidase: biological function. In *Peroxidases in Chemistry and Biology*. J. Everse, K. E. Everse, and M. B. Grisham, eds. CRC Press, Boca Raton, FL, pp. 143–180.
2. Pruitt, K. M. 1987. The salivary peroxidase system: thermodynamic, kinetic, and antibacterial properties. *J. Oral Pathol.* 16: 417–420.
3. Wijkstrom-Frei, C., S. El-Chemaly, R. Ali-Rachedi, C. Gerson, M. A. Cobas, R. Forteza, M. Salathe, and G. E. Conner. 2003. Lactoperoxidase and human airway host defense. *Am. J. Respir. Cell Mol. Biol.* 29: 206–212.
4. Reiter, B., V. M. Marshall, BjörckL, and C. G. Rosen. 1976. Nonspecific bactericidal activity of the lactoperoxidases-thiocyanate-hydrogen peroxide system of milk against *Escherichia coli* and some Gram-negative pathogens. *Infect. Immun.* 13: 800–807.
5. Courtois, P., D. van Beers, M. de Foor, I. M. Mandelbaum, and M. Pourtois. 1990. Abolition of herpes simplex cytopathic effect after treatment with peroxidase generated hypothiocyanite. *J. Biol. Buccale* 18: 71–74.
6. Lenander-Lumikari, M. 1992. Inhibition of *Candida albicans* by the peroxidase/SCN⁻/H₂O₂ system. *Oral Microbiol. Immunol.* 7: 315–320.
7. Gerson, C., J. Sabater, M. Scuri, A. Torbati, R. Coffey, J. W. Abraham, I. Lauredo, R. Forteza, A. Wanner, M. Salathe, et al. 2000. The lactoperoxidase system functions in bacterial clearance of airways. *Am. J. Respir. Cell Mol. Biol.* 22: 665–671.
8. Pruitt, K. M., B. Mansson-Rahemtulla, and J. Tenovou. 1983. Detection of the hypothiocyanite (OSCN⁻) ion in human parotid saliva and the effect of pH on OSCN⁻ generation in the salivary peroxidase antimicrobial system. *Arch. Oral Biol.* 28: 517–525.
9. Linsdell, P., and J. W. Hanrahan. 1998. Adenosine triphosphate-dependent asymmetry of anion permeation in the cystic fibrosis transmembrane conductance regulator chloride channel. *J. Gen. Physiol.* 111: 601–614.
10. Pedemonte, N., E. Caci, E. Sondo, A. Caputo, K. Rhoden, U. Pfeffer, M. Di Candia, R. Bandettini, R. Ravazzolo, O. Zegarra-Moran, and L. J. Galletta. 2007. Thiocyanate transport in resting and IL-4-stimulated human bronchial epithelial cells: role of pendrin and anion channels. *J. Immunol.* 178: 5144–5153.
11. Ferreira, I. M., M. S. Hazari, C. Gutierrez, N. Zamel, and K. R. Chapman. 2001. Exhaled nitric oxide and hydrogen peroxide in patients with chronic obstructive pulmonary disease: effects of inhaled beclomethasone. *Am. J. Respir. Crit. Care Med.* 164: 1012–1015.
12. Geiszt, M., J. Witta, J. Baffi, K. Lekstrom, and T. L. Leto. 2003. Dual oxidases represent novel hydrogen peroxide sources supporting mucosal surface host defense. *FASEB J.* 17: 1502–1504.
13. Dupuy, C., R. Ohayon, A. Valent, M. S. Noel-Hudson, D. Deme, and A. Virion. 1999. Purification of a novel flavoprotein involved in the thyroid NADPH oxidase: cloning of the porcine and human cDNAs. *J. Biol. Chem.* 274: 37265–37269.
14. De Deken, X., D. Wang, M. C. Many, S. Costagliola, F. Libert, G. Vassart, J. E. Dumont, and F. Miot. 2000. Cloning of two human thyroid cDNAs encoding new members of the NADPH oxidase family. *J. Biol. Chem.* 275: 23227–23233.
15. El Hassani, R. A., N. Benfares, B. Caillou, M. Talbot, J. C. Sabourin, V. Belotte, S. Morand, S. Gnidehou, D. Agnandji, et al. 2005. Dual oxidase2 is expressed all along the digestive tract. *Am. J. Physiol.* 288: G933–G942.
16. Grasberger, H., and S. Refetoff. 2006. Identification of the maturation factor for dual oxidase: evolution of an eukaryotic operon equivalent. *J. Biol. Chem.* 281: 18269–18272.
17. Forteza, R., M. Salathe, F. Miot, and G. E. Conner. 2005. Regulated hydrogen peroxide production by Duox in human airway epithelial cells. *Am. J. Respir. Cell Mol. Biol.* 32: 462–469.
18. Moskwa, P., D. Lorentzen, K. J. Excoffon, J. Zabner, P. B. McCray, Jr., W. M. Nauseef, C. Dupuy, and B. Banfi. 2007. A novel host defense system of airways is defective in cystic fibrosis. *Am. J. Respir. Crit. Care Med.* 175: 174–183.
19. Gomez, M. I., and A. Prince. 2007. Opportunistic infections in lung disease: *Pseudomonas* infections in cystic fibrosis. *Curr. Opin. Pharmacol.* 7: 244–251.
20. Price-Whelan, A., L. E. Dietrich, and D. K. Newman. 2006. Rethinking “secondary” metabolism: physiological roles for phenazine antibiotics. *Nat. Chem. Biol.* 2: 71–78.
21. Lau, G. W., D. J. Hassett, H. Ran, and F. Kong. 2004. The role of pyocyanin in *Pseudomonas aeruginosa* infection. *Trends Mol. Med.* 10: 599–606.
22. Reszka, K. J., Y. O’Malley, M. L. McCormick, G. M. Denning, and B. E. Britigan. 2004. Oxidation of pyocyanin, a cytotoxic product from *Pseudomonas aeruginosa*, by microperoxidase 11 and hydrogen peroxide. *Free Radic. Biol. Med.* 36: 1448–1459.
23. Gray, T. E., K. Guzman, C. W. Davis, L. H. Abdullah, and P. Nettekheim. 1996. Mucociliary differentiation of serially passaged normal human tracheobronchial epithelial cells. *Am. J. Respir. Cell Mol. Biol.* 14: 104–112.
24. Leto, T. L., M. C. Lavigne, N. Homoyounpour, K. Lekstrom, G. Linton, H. L. Malech, and I. de Mendez. 2007. The K-562 cell model for analysis of neutrophil NADPH oxidase function. *Methods Mol. Biol.* 412: 365–383.
25. Mahajan-Miklos, S., M. W. Tan, L. G. Rahme, and F. M. Ausubel. 1999. Molecular mechanisms of bacterial virulence elucidated using a *Pseudomonas aeruginosa*-*Caenorhabditis elegans* pathogenesis model. *Cell* 96: 47–56.
26. Dietrich, L. E., A. Price-Whelan, A. Petersen, M. Whiteley, and D. K. Newman. 2006. The phenazine pyocyanin is a terminal signalling factor in the quorum sensing network of *Pseudomonas aeruginosa*. *Mol. Microbiol.* 61: 1308–1321.
27. Cox, C. D. 1986. Role of pyocyanin in the acquisition of iron from transferrin. *Infect. Immun.* 52: 263–270.
28. Harper, R. W., C. Xu, J. P. Eiserich, Y. Chen, C. Y. Kao, P. Thai, H. Setiadi, and R. Wu. 2005. Differential regulation of dual NADPH oxidases/peroxidases, Duox1 and Duox2, by Th1 and Th2 cytokines in respiratory tract epithelium. *FEBS Lett.* 579: 4911–4917.
29. Hartl, D., M. Griese, M. Kappler, G. Zissel, D. Reinhardt, C. Rebhan, D. J. Schendel, and S. Krauss-Etschmann. 2006. Pulmonary T_H2 response in *Pseudomonas aeruginosa*-infected patients with cystic fibrosis. *J. Allergy Clin. Immunol.* 117: 204–211.
30. Muller, M., and T. C. Sorrell. 1997. Modulation of neutrophil superoxide response and intracellular diacylglyceride levels by the bacterial pigment pyocyanin. *Infect. Immun.* 65: 2483–2487.
31. Clark, R. A., K. G. Leidal, and N. S. Taichman. 1986. Oxidative inactivation of *Actinobacillus actinomycetemcomitans* leukotoxin by the neutrophil myeloperoxidase system. *Infect. Immun.* 53: 252–256.

32. Ooi, W., H. G. Levine, J. T. LaMont, and R. A. Clark. 1984. Inactivation of *Clostridium difficile* cytotoxin by the neutrophil myeloperoxidase system. *J. Infect. Dis.* 149: 215–219.
33. Machen, T. E. 2006. Innate immune response in CF airway epithelia: hyperinflammatory? *Am. J. Physiol.* 291: C218–C230.
34. Campodonico, V. L., M. Gadjeva, C. Paradis-Bleau, A. Uluer, and G. B. Pier. 2008. Airway epithelial control of *Pseudomonas aeruginosa* infection in cystic fibrosis. *Trends Mol. Med.* 14: 120–133.
35. Leto, T. L., and M. Geiszt. 2006. Role of Nox family NADPH oxidases in host defense. *Antioxid. Redox Signal.* 8: 1549–1561.
36. Schwarzer, C., T. E. Machen, B. Illek, and H. Fischer. 2004. NADPH oxidase-dependent acid production in airway epithelial cells. *J. Biol. Chem.* 279: 36454–36461.
37. Shao, M. X., and J. A. Nadel. 2005. Dual oxidase 1-dependent MUC5AC mucin expression in cultured human airway epithelial cells. *Proc. Natl. Acad. Sci. USA* 102: 767–772.
38. Conner, G. E., C. Wijkstrom-Frei, S. H. Randell, V. E. Fernandez, and M. Salathe. 2007. The lactoperoxidase system links anion transport to host defense in cystic fibrosis. *FEBS Lett.* 581: 271–278.
39. Wilson, R., D. A. Sykes, D. Watson, A. Rutman, G. W. Taylor, and P. J. Cole. 1988. Measurement of *Pseudomonas aeruginosa* phenazine pigments in sputum and assessment of their contribution to sputum sol toxicity for respiratory epithelium. *Infect. Immun.* 56: 2515–2517.
40. Strausbaugh, S. D., and P. B. Davis. 2007. Cystic fibrosis: a review of epidemiology and pathobiology. *Clin. Chest Med.* 28: 279–288.
41. Thomassen, M. J., C. A. Demko, J. D. Klinger, and R. C. Stern. 1985. *Pseudomonas cepacia* colonization among patients with cystic fibrosis: a new opportunist. *Am. Rev. Respir. Dis.* 131: 791–796.
42. O'Malley, Y. Q., K. J. Reszka, D. R. Spitz, G. M. Denning, and B. E. Britigan. 2004. *Pseudomonas aeruginosa* pyocyanin directly oxidizes glutathione and decreases its levels in airway epithelial cells. *Am. J. Physiol.* 287: L94–L103.